

Single-Input-Multiple-Output Wi-Fi Radar for Vital Signal Sensing and Device Tracking

Xianjun Jiao, Thijs Havinga, Wei Liu and Ingrid Moerman

IDLab - imec, Ghent University, Belgium

{firstname.lastname}@imec.be

Abstract—Multiple Input Multiple Output (MIMO) radar systems enhance detection and anti-interference capabilities by increasing the number of antennas compared to traditional radar systems. Despite significant research into Wi-Fi sensing in recent years, constructing Wi-Fi MIMO radar remains challenging due to half-duplex RF hardware and limited access to low-level multi-antenna signals in commercial Wi-Fi chips. This paper presents a SIMO Wi-Fi radar with one Tx and two Rx antennas, based on the open-source Wi-Fi SDR platform, openwifi, which has implemented the full 802.11 stack. The hardware includes an FPGA and an AD9361 RF front-end. Directional antennas are used to reduce Tx-Rx interference in full-duplex mode. This Wi-Fi MIMO radar system brings dual capabilities: sensing the passive target that is not transmitting any signals and the normal Wi-Fi device that transmits signals for data traffic. In this paper, the dual capabilities are demonstrated in two cases: vital signal sensing for humans and Angle of Arrival (AoA) tracking of another device. More specifically, millimeter-level movement detection is achieved by processing phase information from the Channel State Information (CSI) of the two Rx antennas.

Index Terms—Wi-Fi, Radar, CSI, sensing, SDR, 802.11

I. INTRODUCTION

Radar and MIMO radar [1] have been extensively studied for sensing. A typical Frequency Modulated Continuous Wave radar [2] operates in full-duplex mode, using directional antennas and circulator to prevent receiver saturation. Integrating sensing into wireless communication systems is a hot topic and expected to be crucial for next-generation mobile and Wi-Fi systems.

Besides radar, Wi-Fi based sensing methods [3] have been proposed for vital signal detection, pose recognition, and localization. Unlike radar systems, Wi-Fi operates in half-duplex mode, so the receiver is always working on incoming signals from other nodes. The difference between local oscillators of transmitter and receiver pose challenges to signal processing, data collection, and system design.

In this paper, we address the challenges of integrating radar into Wi-Fi systems by implementing a SIMO radar system on the openwifi [4] SDR platform. The standard Wi-Fi OFDM waveform is used for both communication and sensing. Joint communication and sensing are achieved by performing normal Wi-Fi communication in half-duplex and radar processing during self-transmission by keeping the receiver always on. The receiver is programmed to synchronize the Tx time-frequency instead of estimate it during reception. By processing signals from two Rx antennas, we demonstrate

the human's breath detection in radar mode and AoA tracking of other devices, together with normal Wi-Fi communication.

The differences between this work and [5] are: The setup of [5] is based on our "WiFi CSI radar" application note released in 2022 on Github of [4]; [5] uses time-domain Channel Impulse Response based algorithm, we use phase difference based on frequency-domain CSI. Furthermore, we demonstrate the AoA tracking, which is not in [5].

II. THE SYSTEM MODEL AND ALGORITHMS

A. The monostatic SIMO Wi-Fi radar

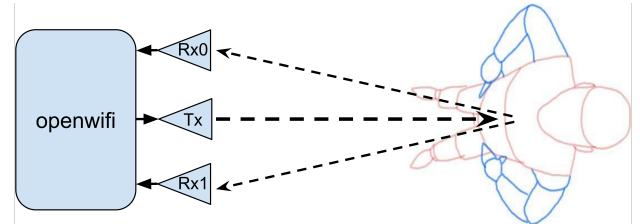


Fig. 1: The monostatic SIMO Wi-Fi radar for breath sensing

Fig. 1 shows the principle of monostatic SIMO radar in the breath detection scenario, where the Tx signal reflects via the human body to the receiving antennas Rx0 and Rx1. For simplicity, multi-path is not present in the following equations, only a single path is considered. In case of the multipath in the real world, the paths can be separated via Inverse Discrete Fourier Transform (IDFT) of the frequency domain channel response (also known as CSI), and the following analysis is still valid per path. Eq. (1) is the baseband form of one transmitted OFDM symbol, where T_{sym} is the symbol duration, k is the subcarrier index, f_k is the RF frequency of the subcarrier k , a_k and θ_k are amplitude and phase due to the modulation on the subcarrier k .

$$s(t) = \sum_{k=0}^{K-1} a_k e^{j(2\pi f_k t + \theta_k)}, 0 < t \leq T_{\text{sym}} \quad (1)$$

Eq. (2) is the received OFDM symbol on Rx0, where b_k^0 is the combined gain of Tx-Rx hardware and the wireless channel. The RF frequency f_k of the subcarrier k is exactly the same as in the transmitter because Tx and Rx share the same local oscillator which leads to no Carrier Frequency Offset (CFO). T is the sample time. The hardware delay

is static, and can be represented by two parts: the part nT represents integer multiples of the sample time and the part ΔT_{fix}^0 is in fractional sample time. ΔT_{ch}^0 is the over-the-air delay from Tx to body, then to Rx0. $\Delta T_{\text{ch}}^0 = d^0/c$, where d^0 is the total distance and c is the speed of light.

$$r^0(t) = \sum_{k=0}^{K-1} b_k^0 a_k e^{j(2\pi f_k(t-nT-\Delta T_{\text{fix}}^0-\Delta T_{\text{ch}}^0)+\theta_k)} \quad (2)$$

In the receiver baseband, nT is removed by proper FFT window offset. The correct n can be decided by calibration and fixed during the sensing operation. In the calibration phase, the time is marked when the 1st IQ sample of the Wi-Fi packet starts transmission in the baseband transmitter, and the receiver detects the Long Training Field (LTF) in the received Wi-Fi signal. Then n can be calculated by counting how many samples have passed in the receiver from the marked time in the transmitter till the LTF is detected in the receiver. Eq. (3) is the phase term on subcarrier k taken from (2). Eq. (4) is the phase difference between the two receive antennas.

$$\angle r_k^0 = -\Delta T_{\text{fix}}^0 2\pi f_k - \Delta T_{\text{ch}}^0 2\pi f_k + \theta_k \quad (3)$$

$$\angle r_k^1 - \angle r_k^0 = (\Delta T_{\text{fix}}^0 - \Delta T_{\text{fix}}^1) 2\pi f_k + \left(\frac{d^0 - d^1}{c} \right) 2\pi f_k \quad (4)$$

In (4), the 1st term is constant (hardware property). The 2nd term $d^0 - d^1$ changes along with the target move. With Wi-Fi channel 40 (5200MHz), the 1st subcarrier is at $5200 \text{ MHz} - 26 \times 0.3125 \text{ MHz} = 5191.875 \text{ MHz}$ (20MHz 802.11a). With 1 mm change of $d^0 - d^1$, the phase change will be $(1 \text{ mm}/c) \times 2\pi \times 5191.875 \text{ MHz} = 0.11 \text{ rad}$, which is 6.23° . It can be detected easily by modern high quality RF and baseband hardware as shown in section III. Multiple subcarriers can be averaged to reduce noise and improve the detection performance further.

Notice that the above measurement can be done based on a single Wi-Fi packet. Openwifi has FPGA time stamping with 10ns resolution for every transmitted packet. If short packet is used, the openwifi platform can send out Wi-Fi packet every 1ms on average. By monitoring the phase change of different received/reflected-back packet at different time stamps, Doppler frequency caused by the target movement can be derived.

B. AoA estimation

Due to the openness of the wireless medium, the Wi-Fi receiver can receive all the Wi-Fi packets from other devices in the same/current channel even the packets are not intended for this receiver, so other devices can be tracked by AoA estimation. In this case, the Eq. (2) becomes Eq. (5), where Δf^0 and $n^0 T$ are the CFO (because of the slight difference between the transmitter and receiver local oscillators) and integer sample delay of Rx antenna 0. In case of AD9361 RF front-end, the antenna 1 signal has the same CFO: $\Delta f^1 = \Delta f^0$ due to the common local oscillator of

two Rx chains. After CFO estimation and correction in the receiver, the residual CFO is noted as Δf . The integer sample delay of antenna 1 is also the same: $n^1 = n^0$, because one sample delay difference (50ns in case of 20Msps) means the distance difference of 15m which is not possible when two Rx antennas are closely located.

Following the similar principle in section II-A, the phase difference between Rx0 and Rx1 is derived in (6). The 1st term is static and can be removed by calibration, then the 2nd term can be measured (d^0 and d^1 are the distance from the device under tracking to two Rx antennas). AoA can be calculated based on $d^0 - d^1$ if the antenna spacing is known. Δf can be ignored because it is much less than f_k : As a rule of thumb and common practice of all OFDM receivers, CFO estimation and compensation ensure the residual CFO Δf is less than 1 percent of the OFDM subcarrier spacing, so that the Inter Carrier Interference (ICI) is small enough. The subcarrier spacing is 312.5kHz before 802.11ax, so the Δf is less than 3.125kHz. As comparison, f_k is in the order of several thousands MHz in the analysis in section II-A.

$$r^0(t) = \sum_{k=0}^{K-1} b_k^0 a_k e^{j(2\pi(f_k+\Delta f^0)(t-n^0 T-\Delta T_{\text{fix}}^0-\Delta T_{\text{ch}}^0)+\theta_k)} \quad (5)$$

$$(\Delta T_{\text{fix}}^0 - \Delta T_{\text{fix}}^1) 2\pi(f_k + \Delta f) + \left(\frac{d^0 - d^1}{c} \right) 2\pi(f_k + \Delta f) \quad (6)$$

III. THE EXPERIMENT SETUP AND RESULTS

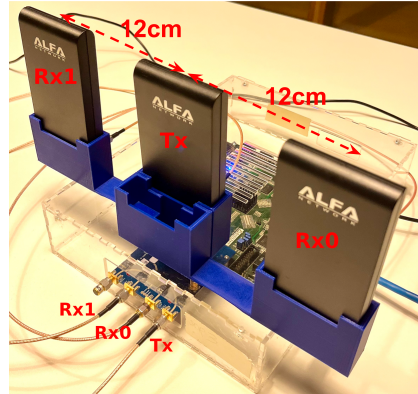


Fig. 2: The openwifi SIMO experimental platform for sensing

Utilizing the source code of the openwifi SDR platform, algorithms in section II are implemented to realize the breath monitoring and device tracking in the experiments.

Fig. 2 illustrates the hardware setup and antenna topology used in the experiment. It is composed by Zedboard, AD-FMCOMMS2-EBZ and 3 dual-band directional panel antennas (model: APA-M25 from ALFA Network Inc). To extend to 4 Rx antennas, AD-FMCOMMS2-EBZ needs to be upgraded to AD-FMCOMMS5-EBZ.

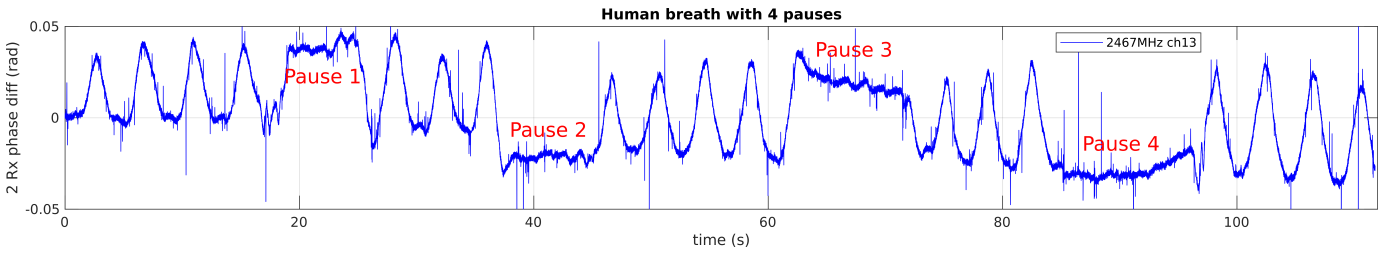


Fig. 4: Phase difference while a human breathes with 4 pauses.

A. Breath monitoring in radar mode

Fig. 3 presents snapshots of the real-time phase difference between the two Rx antennas while a human breathes 61 cm in front of the radar during two 24 second experiments in an office: one conducted on Wi-Fi channel 13 (2472MHz, blue) and the other on channel 40 (5200MHz, red). The measurement rate is approximately 700 packets per second. Since the 5 GHz wavelength is about half that of the 2.4 GHz wavelength, the red curve exhibits a larger phase change. In the figure, the 0.15 rad phase difference change (red) at 5200 MHz (wavelength 57.7 mm) indicates that the $d^0 - d^1$ distance change is approximately 1.37 mm.

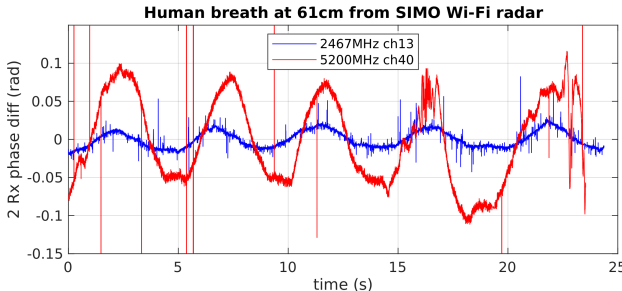


Fig. 3: Rx0 Rx1 Phase difference while a human breathes

The sensing results are further validated by comparing to the ground truth respiratory rate, which is counted by the people under sensing. The sensed rate is well aligned with the actual rate. If the people actively hold his breath, the breath pausing can be identified clearly in the data playback as shown in Fig. 4, where 4 pauses are observed. The small variants during the pause might relate to the heart beat.

B. Device tracking by AoA estimation

The real-time phase difference between signals received by two Rx antennas is in Fig. 5 (left half, polar coordinates).

The measurable phase difference can be as low as 0.1 rad (actually it even achieves 0.05 rad in case of the blue curve in Fig. 3). In Fig. 5 (right), half-wavelength Rx antenna spacing is assumed, and the target is in the area directly in front of the antennas and not off the center axis far. The calculation of the AoA in accordance to 0.1 rad phase difference is in (7), where λ is wavelength. The result shows resolution better than 2° .

$$\begin{aligned} \text{Angle}^\circ &= \frac{180}{\pi} \times \text{atan} \left(\frac{d^0 - d^1}{\text{antenna_spacing}} \right) \\ &= \frac{180}{\pi} \times \text{atan} \left(\frac{\lambda \times 0.1 \text{rad}/(2\pi)}{\lambda/2} \right) = 1.82^\circ \end{aligned} \quad (7)$$

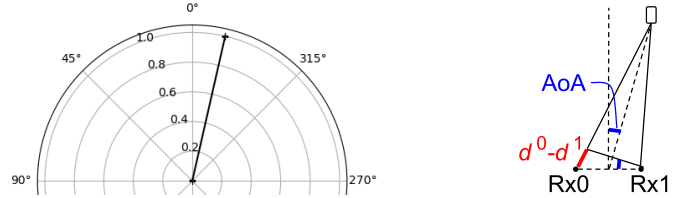


Fig. 5: AoA estimation of other Wi-Fi device

IV. CONCLUSION

A SIMO radar can be constructed using standard Wi-Fi systems with full-duplex operation and multi-antenna signal access. The phase difference calculation algorithm is demonstrated achieving movement detection resolution on the order of millimeters. This capability enables effective breath monitoring and AoA tracking.

ACKNOWLEDGMENT

This work is funded by 6G-MUSICAL EU Horizon Grant Agreement No. 101139176, Belgium FWO SBO SMARTSTRIP Grant S006224N and Belgian Defense through Contract No. 22DEFRA004 (DEFRA-BOLSTER project).

REFERENCES

- [1] D. W. Bliss and K. W. Forsythe, "Multiple-input multiple-output (MIMO) radar and imaging: degrees of freedom and resolution," The 37th Asilomar Conference on Signals, Systems & Computers, Pacific Grove, CA, USA, 2003, pp. 54-59, 2003
- [2] G. Wang, C. Gu, T. Inoue and C. Li, "A Hybrid FMCW-Interferometry Radar for Indoor Precise Positioning and Versatile Life Activity Monitoring," IEEE Transactions on Microwave Theory and Techniques, vol. 62, no. 11, pp. 2812-2822, 2014
- [3] J. Liu, H. Liu, Y. Chen, Y. Wang and C. Wang, "Wireless Sensing for Human Activity: A Survey," IEEE Communications Surveys & Tutorials, vol. 22, no. 3, pp. 1629-1645, 2020
- [4] X. Jiao, W. Liu, M. Mehari, M. Aslam and I. Moerman, "openwifi: a free and open-source IEEE802.11 SDR implementation on SoC," 2020 IEEE 91st Vehicular Technology Conference (VTC2020-Spring), Antwerp, Belgium, pp. 1-2, 2020
- [5] A. T. Kristensen, S. Li, A. Balatsoukas-Stimming and A. Burg, "Monostatic Multi-Target Wi-Fi-Based Breathing Rate Sensing Using Openwifi," 2024 IEEE Wireless Communications and Networking Conference (WCNC), Dubai, United Arab Emirates, pp. 1-6, 2024